A Polarization Reconfigurable Patch Antenna in the Millimeter-Waves Domain Using Optical Control of Phase Change Materials

Jehison Leon Valdes, Laure Huitema, Eric Arnaud, Damien Passerieux, Aurelian Crunteanu

Received 6 April 2020; revised 10 May 2020; accepted 17 May 2020. Date of publication 22 May 2020; date of current version 11 June 2020.

Digital Object Identifier 10.1109/OJAP.2020.2996767

A Polarization Reconfigurable Patch Antenna in the Millimeter-Waves Domain Using Optical Control of Phase Change Materials

JEHISON LEON VALDES, LAURE HUITEMA (Member, IEEE), ERIC ARNAUD, DAMIEN PASSERIEUX, AND AURELIAN CRUNTEANU (Member, IEEE)

XLIM Research Institute/UMR CNRS 7252, University of Limoges, 87000 Limoges, France

CORRESPONDING AUTHOR: J. L. VALDES (e-mail: jehison.leon@xlim.fr)

This work was supported in part by the France Region Limousin and in part by the National Authority for Scientific Research (ANCS)-Romania, under the H2020 European project MASTERS (https://www.unilim.fr/h2020_masters/).

ABSTRACT We present the integration of GeTe (Germanium Telluride), a phase change material (PCM), within the structure of an antenna operating in the millimeter wave domain (∼ 30 GHz) in order to make it reconfigurable in three polarizations: a linear polarization (LP), a left hand circular polarization (LHCP) and a right hand circular polarization (RHCP). The device is based on a conventional patch antenna excited by a microstrip line with the GeTe material integrated into the four corners of the patch. The phase change between the insulating (OFF) and metallic (ON) states of this material is controlled by direct irradiation using ultraviolet (UV) short laser pulses and allows the reconfigurability of the antenna between an LP, an LHCP and an RHCP. The measured performances of the fabricated device show axial ratios of less than 3 dB over a 400 MHz of bandwidth around 29.5 GHz with total efficiencies up to 75 % for the circularly polarized configurations and a maximum gain up to 8.3 dBi for the linear polarization states.

INDEX TERMS Optical activation, patch antenna, phase change material, polarization reconfiguration.

I. INTRODUCTION

IN RECENT years, the increase in data traffic and the rapid development of wireless communication technologies have increased the interest in designing more compact antenna systems with reconfigurability functions (frequency, radiation pattern and/or polarization) [1]–[4]. The maximum transmitted power between two emission/reception systems is obtained when communicating antennas use identical polarizations, either linear (vertical or horizontal) or circular (left or right) polarizations. Many military and space applications require circular polarization, which can also be an interesting solution in the civil domain to overcome misalignment between transmitter and receiver and to mitigate inherent polarization loss factors due to multipath losses [5]. Circular polarization can also overcome the effects of deflections, propagation and ground reflections for satellite applications.

Therefore, reconfigurable polarization antennas, namely, antennas that change between circular (left- and right-hand) and linear polarizations, allow devices to adapt their radiation characteristics to variable environments and improve the quality and the robustness of the wireless link. In addition, the polarization reconfigurability in a device allows frequency reuse, which extends the system's capabilities, and becomes useful when the operating frequency band is limited [6].

One method for obtaining circular polarization in an antenna is to use a feeding technique (single or multiple) exciting two linearly polarized orthogonal modes with a phase difference of 90° [8]–[10]. It is also possible to obtain circular polarization by integrating disturbance zones in the antenna design [5]–[7] or by using magnetic materials [11].

Polarization reconfigurability has been studied in the literature [5], [6], [8] and offers solutions based on PIN diodes or MEMS, i.e., with a continuous electrical polarization. In this work, we propose a polarization reconfigurable antenna using the optical control of specific elements integrated within the antenna main body realized with phase change material (PCM). PCM-based technology has been recently proven to be an effective method for realizing high-frequency switches (including the millimeter-waves frequencies) by controlling the material's properties (from an insulating state to a metallic one) using optical or electrical excitations [12]–[22].

The integration of GeTe or GST ($Ge_2Sb_2Te_5$) phase change materials into high-frequency functions is based on their ability to change from an amorphous state, OFF (insulating phase material) to a crystalline state, ON (conductive phase material) following the application of a thermal, electrical or optical stimulus. These materials have a good power handling capability, low energy consumption, high OFF state isolation, low ON state losses and a factor of merit greater than the current semiconductor-based switching technologies, over large frequency domains (up to 70 GHz) [12]–[22]. The key advantage of PCM-based devices technology is the bi-stability, i.e., they do not require a permanent bias to be maintained in their ON or OFF state. Often investigated and integrated in high-frequency devices and coined as a phase change material, the vanadium dioxide (VO_2) (presenting also a thermal-, electronic- or optical-triggered metal-insulator transition (MIT)) is inherently different from PCMs with respect of its volatile-type transition. Typically, at room temperature, VO_2 is a low bandgap semiconductor while above the critical transition temperature of ∼68 °C, it transform to a metal. In order to keep the VO_2 in its metallic state, a continuous energy input (thermal, electrical, optical) is required, while the advantage of PCM-based materials (such GeTe) and associated devices over the VO_2-based solutions is that they are providing a latching metallic/ ON state and do not require continuous energy intake for maintaining it (bi-stability or non-volatile-type behavior) [23], [24].

PCMs transformation from an amorphous to a crystalline state and inversely, requires controlled and precise heating and cooling conditions brought by optical or electrical activation [12]–[16]. Compared with previously reported electrical activation of phase change in GeTe materials requiring elaborate heating scheme and technologically- complexmaterial stacks (thin film resistors, thermal and dielectric barriers, PCM-active and passivation materials) [14]–[16], optical activation of PCMs materials [20]–[22] and high frequency devices [12], [13], using direct irradiation with short optical pulses, may be preferable from the point of view of device fabrication simplicity and its non-essential encapsulation/ packaging requirements.

For antenna's applications, the optical control of PCMs with short laser pulses is significantly reducing the device's switching time (few nanoseconds), is avoiding complex manufacturing and the integration of polarization (bias) lines otherwise required for PCM's electrical activation, which may introduce parasitic and disturbances of the antenna's radiation pattern.

Here, we propose for the first time a polarization reconfigurable antenna which is designed as a square metal patch excited by a microstrip line and incorporating a phase change material (GeTe) on each corner. The phase change of these GeTe patterns, between their insulating (OFF) and metallic (ON) states, is realized using direct laser irradiation [12], [13]. This will modify the overall geometry of the patch and, depending on the specific state of the GeTe elements, will allow the antenna to operate, repeatedly, with a left hand circular polarization (LHCP), a right hand circular polarization (RHCP) or even a linear polarization (LP).

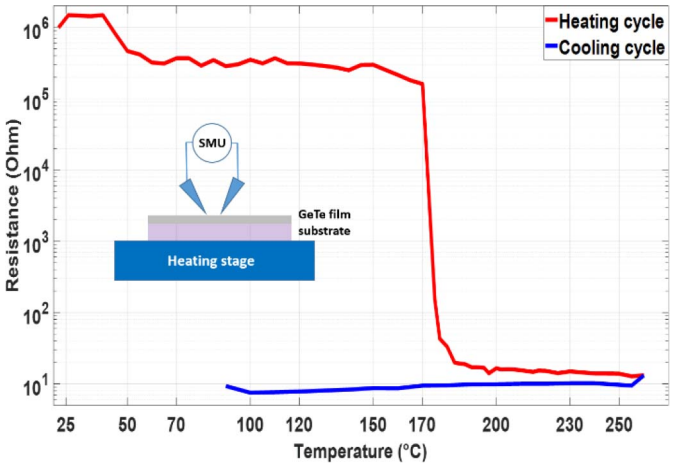

FIGURE 1. Resistance variation with temperature during a direct heating cycle of a 1-μm thick GeTe layer obtained on a sapphire substrate.

In the following, we will present the properties of the GeTe material and its phase changes using thermal and optical control, and the evaluation of the electrical properties of this material in the millimeter wave domain. In a second part, we will use these GeTe properties to design the polarization reconfigurable antenna device using the optical control of GeTe elements integrated with the main metallic patch. Finally, following the device fabrication, we will evaluate its performances and compare the simulations with the experimental results.

II. ELECTRICAL PROPERTIES AND OPTICAL CONTROL OF GETE

The significant variations in resistivity of PCM during insulating-to metallic phase change (5-6 orders of magnitude) can be obtained over very wide frequency domains, from DC to THz waves. Preliminary tests of the GeTe material were carried out on alumina, sapphire and silica substrates. The temperature-dependent electrical resistance variation of the GeTe was determined using two-probe measurement, spaced by 1 mm, on 1-thick μm thin layers deposited directly by DC magnetron sputtering on sapphire substrates using a 50:50 (weight %) GeTe target. The GeTe films, initially obtained in the amorphous phase (insulating state), were transformed into their crystalline phase (conductive state) by applying a direct heating cycle in air (from 23°C to 260°C, with a ramp of 5°C/min)) followed by cooling to room temperature. The temperature dependent resistance of the film was recorded in air using an electrical set-up depicted as an insert in Fig. 1 (two electrical probes connected to a source-measurement unit (SMU).

As shown in Fig. 1, during the heating cycle, the GeTe undergoes a sudden and irreversible change of its resistance towards the metallic phase at ∼170°C (crystallization temperature), with a decrease in resistance of six orders of magnitude. During the cooling cycle, the material retains its

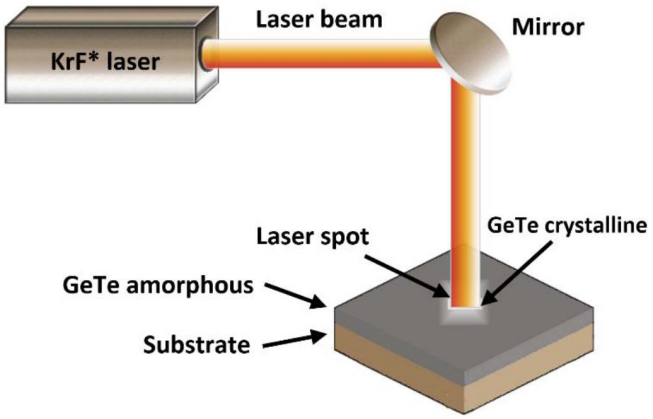

FIGURE 2. Laser irradiation scheme of a GeTe layer.

crystalline state of low resistance (bi-stability). The absolute values of the DC resistances in the two states depend on the distance between the DC points.

The material can be placed in the crystalline/metallic state either by direct heating using a heating plate (like the process shown on Figure 1), by Joule direct- or indirect- heating using short current pulses (as currently employed for non-volatile memory technologies or RF-PCM switches [14]–[16]) or by direct laser irradiation using short laser pulses which will locally heat the material in a controlled way [13], [20]–[22]. Subsequently, the reversible transition from a metallic to an insulating state can be achieved, in a repetitive and reproducible manner, by using the direct irradiation of the GeTe film with short laser pulses, with a KrF Compex Pro110 laser ($\lambda = 248$ nm, 15 mm x 5 mm laser spot size, a pulse duration of $\sim$30 ns and pulse peak powers in the kW-MW range), as shown in Fig. 2. Our preliminary investigations using an electrical probing scheme during optical irradiation of the GeTe layer show switching times from the amorphous-to crystalline state in the order of 40-50 ns which are consistent with previous studies on switching processes with very short laser pulses [21].

In order to evaluate the electrical properties of GeTe in the millimeter wave domain, the material (1-μm thick) was integrated into a coplanar waveguide (CPW) structure and within a frequency agile patch antenna, both on an alumina substrate (400 μm thick) [12]–[13].

As previously demonstrated, the crystallization of GeTe requires a single laser pulse (LP1) with a fluence (laser surface energy density) between 85 and 90 mJ/cm^2. The amorphisation of the material is carried out with a second laser pulse (LP2) having a much higher fluence, between 185 and 190 mJ/cm^2. The size of the laser beam (15 mm x 5 mm) allows the successive and repetitive switching between the two phases of the material not only over large areas but also on localized areas using proximity masks [13].

Based on our previous reports on GeTe integration in RF-GeTe switches and GeTe-based antenna [12]–[13], we extracted the GeTe layers performances in the 20-60 GHz frequencies range (permittivity, conductivity) in both amorphous and crystalline states by comparing the experimental results and the 3D electromagnetic simulations of these specific devices using CST Studio Suite. The two GeTe phases were afterwards created in the CST Studio Suite database as new materials having specific permittivity and conductivities. Thus, the films of GeTe prepared in the crystalline state have a conductivity between 3.5 x 10^5 and 4 x 10^5 S/m and the amorphous state between 3 and 10 S/m with a permittivity of 70. These GeTe characteristics have been used to design and demonstrate the polarization-tunable patch antenna in the millimeter wave domain.

This specific optical operation mode (using a rather massive excimer laser) can be perceived as difficult to implement for practical reconfigurable antenna applications, since for in-situ operation it would require precise alignment of the laser beam with the GeTe areas to be optically modified and integrated into the antenna topology. However, as demonstrated henceforth, the integration versatility of GeTe bi-stable films forming part of the radiating element of the antenna and its optical activation (without the need of complex technological steps and packaging), together with the novel proposed design of the polarization reconfiguration antenna, may provide beneficial insights to the antenna community towards the design of multifunctional antennas and reconfigurable systems based on PCM technology. Moreover, it was already shown [22] that it is possible to drastically reduce the optical irradiation set-up imprint for a more integrated, (possible in-situ operation setup) using appropriate infrared diode laser radiation conveyed by optical fibers in the vicinity of the PCM areas to be optically activated between the two states. Several other optical-based solutions with a higher degree of integration may, most probably, rise in the future, providing that the phase change materials device implementation will be validated as a convenient, low-power consumption, high-bandwidth tunable element.

III. DESIGN OF THE POLARIZATION TUNABLE PATCH ANTENNA

The topology of the proposed antenna is based on a single feed square metal patch (2.5 mm x 2.5 mm) fabricated on a RO4003C substrate of 12.5 mm x 12.5 mm, with a thickness of 0.305 mm, a dielectric permittivity of $\varepsilon_r = 3.38$ and a loss tangent of $\tan\delta = 0.0027$, to operate around 30 GHz.

Four truncated corners having an equal side length (S = 0.45 mm) are cut and replaced by GeTe patterns as shown in Fig. 3 [6], [26]. A cross-slot (X-slot) pattern is also etched away from the center of the square patch and replaced by the amorphous GeTe material in order to improve the bandwidth of the antenna ($|S_{11}| < -10$ dB) and the axial ratio bandwidth of the circular polarization (AR $<$ 3dB). Within this configuration, the antenna presents a linear polarization when the four GeTe corners are all in the same state (insulating or metallic). The operating frequency of the device is around 30.4 GHz when the four corners in GeTe are amorphous and around 29.5 GHz when they are crystalline. Changing

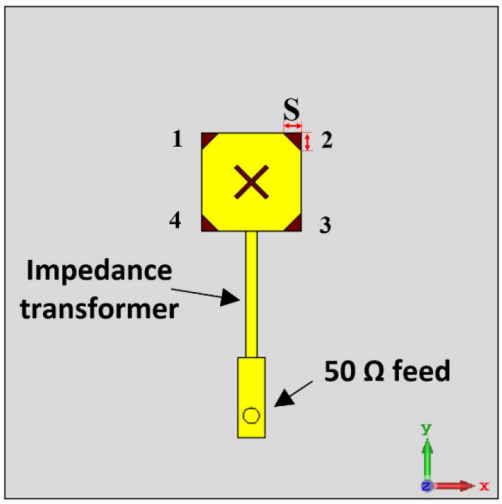

FIGURE 3. Front view of the 3D design of the patch antenna. The GeTe material is represented by the brown-colored corners around the main metallic patch and within the etched cross-slot in the center of the patch.

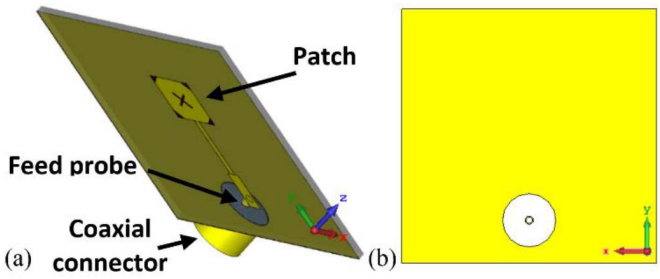

FIGURE 4. (a) 3D design of the patch antenna. (b) Bottom view.

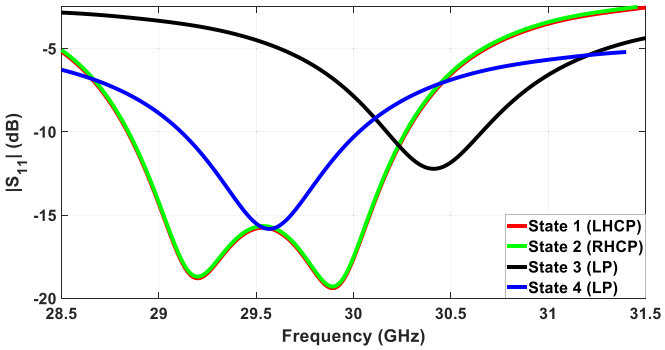

FIGURE 5. Simulations results of $|S_{11}|$ for different operating configurations of the antenna corresponding to the GeTe pattern states indicated in Table 1.

TABLE 1. Polarization configurations of the antenna for four combinations of GeTe states and their operation frequencies.

State	Corner 1	Corner 2	Corner 3	Corner 4	Polar.	Freq. (GHz)
1	OFF	ON	OFF	ON	LHCP	29.5
2	ON	OFF	ON	OFF	RHCP	29.5
3	OFF	OFF	OFF	OFF	LP	30.4
4	ON	ON	ON	ON	LP	29.5

the symmetry of the antenna, for instance, by activating two opposite GeTe corners in the metallic state while keeping the other two in the insulating state, will allow the installation of two orthogonal degenerated modes (TM_{01} and TM_{10}) at the same resonance frequency and, consequently, a circular polarization operation.

The width and length of the cross-slot can be conveniently adjusted for shifting the central frequency of the axial ratio bandwidth in order to overlap it with the impedance matching bandwidth. Thus, the dimensions of this slot were optimized, in order to superpose the center frequencies of the axial ratio bandwidth and of the antenna impedance bandwidth in order to have identical operating frequencies (frequency reuse) for the different prepared polarizations (LP, RHCP and LHCP). A quarter-wavelength transformer with a characteristic impedance of 83 Ω is added in order to match the input impedance of the patch with the 50-Ω microstrip feed line. This latter is excited by a coaxial connector (conveying a feeding probe) through the ground plane and the substrate, as shown in Fig. 4.

The overall topology of the structure can be tuned, by optically preparing the different configurations (ON / OFF) of the PCM material patterns. The different operating polarizations states of the antenna depending on the GeTe patterns configurations are shown in Table 1. Thus, in the cases where the GeTe patterns of the corners 2 and 4 are in the crystalline state and the corners 1 and 3 in the amorphous state, a left-hand circular polarization (LHCP) is obtained (State 1). Conversely, when the corners 1 and 3 are in the crystalline state and the corners 2 and 4 in the amorphous state, a right-hand circular polarization (RHCP) is established (State 2). Finally, when the physical structure of the antenna has all its corners in its OFF or ON states (States 3 and 4), due to its geometrical symmetry, it exhibits a linear polarization (LP) along the Y-direction in the both LP states.

Other factors, including the dielectric permittivity and the thickness of the substrate, the size of the disturbance patch zones (dimensions of the cross-slot), as well as the total size of the antenna, also influence the performance of the circular polarization in the device. Fig. 5 presents the simulated $|S_{11}|$ parameters (using the 3-D electromagnetic solver CST Studio Suite) for the four configurations represented in Table 1. Since the antenna configurations in state 1 and state 2 have exactly the same geometrical symmetry, the RHCP and the LHCP have similar performances with respect to operating frequency, return loss, gain and AR, which is an ideal feature for applications where polarization reconfiguration is required. Due to this symmetry, the following paragraphs (radiation properties analysis) will focus on State 1 (LHCP), taking into account that State 2 (RHCP) show identical simulation performances (ideal case) and very similar measurement performances (as discussed in the next section). As also observed from Fig. 5, the impedance matching bandwidth of the configuration in the State 3 (all the

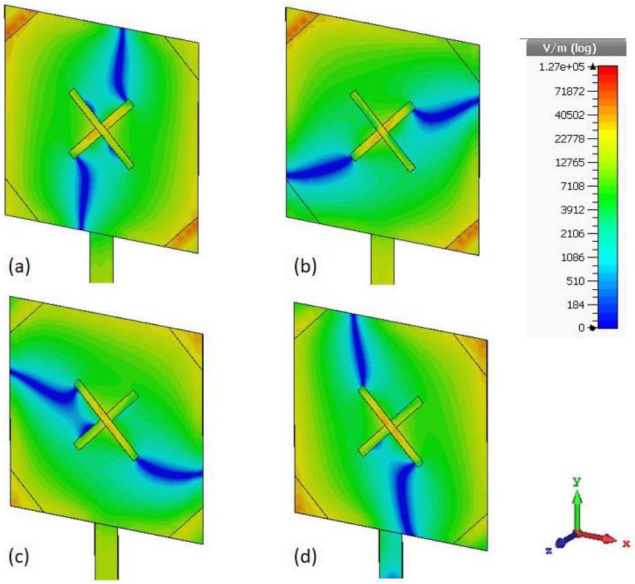

FIGURE 6. Simulated E-field distribution on patch antenna in State 1 at 29.5 GHz for (a) phase = 0°, (b) phase = 45°, (c) phase = 90° and (d) phase = 135°.

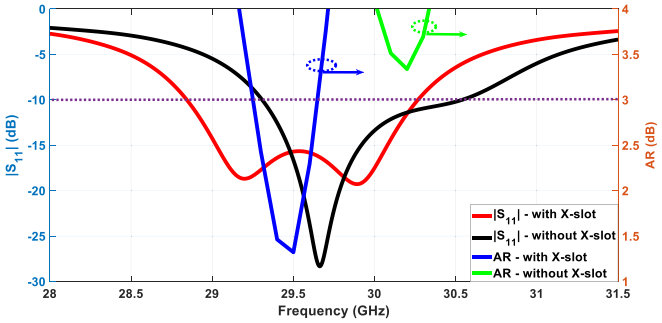

FIGURE 7. Simulations results of $|S_{11}|$ and AR of the antenna with and without cross-slot for the configuration corresponding to the State 1 of the antenna (LHCP).

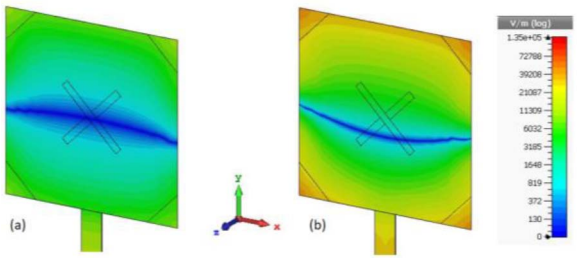

FIGURE 8. Simulated E-field distribution on the patch antenna in State 4 at 29.5 GHz for (a) phase = 0°, (b) phase = 90°.

GeTe patterns are amorphous) is shifted at higher frequencies with respect to the circular polarization (States 1 and 2) and to the linear polarization configuration in the State 4 (when all the GeTe corner patterns are crystalline), due to the globally lower dimensions of the overall hybrid patch in this specific State 3 case. Since our objective is to obtain a polarization reconfigurability for a same frequency band around 29.5 GHz, we will only analyze the performances of State 4 in the case of the linear polarization operation.

Fig. 6 shows the simulated results of the E-field phase distribution for the antenna in State 1 at 29.5 GHz. It can be seen from the directions of the E-field distribution at four different phase values that the antenna radiates a LHCP wave in this configuration.

Several reports in the literature explained that the use of a slot etched within the radiating element of the antenna can improve its performance [26]–[29]. This X-type slot (X-slot) having optimized dimensions (1-mm length and 0.1-mm width), provide a capacitance that can balance the inductance coming from the vertical feeding probe and thus, is improving the impedance and axial-ratio bandwidths. A study on its influence on the circular polarization state of the antenna is shown on Fig. 7 showing the simulated $|S_{11}|$ and AR parameters of the antenna with and without the X-slot. From the simulation results, it can be concluded that even if the antenna has a good matching bandwidth in both cases, the minimum value of AR is found to occur with the presence of the slot. It is clearly seen that the presence of the X-slot gave a significant improvement of the AR bandwidth, while slightly enhanced the impedance bandwidth.

From the simulated E-field distribution of Fig. 8, it can be seen that in the configuration corresponding to the State 4 antenna radiates an LP wave at 29.5 GHz.

In summary, the simulated performances of the antenna show a −10 dB impedance bandwidth of 5.1 % for the CP and 3.1 % for the LP in State 4. The 3-dB bandwidth of AR in CP is 1.7 %. A total efficiency of 83 % for the CP and 74 % for the LP are found at 29.5 GHz, frequency where the minimum of $|S_{11}|$ occurs in the LP operation and where the minimum of AR is found in CP operation.

IV. PROTOTYPING AND MEASUREMENT OF THE ANTENNA DEVICE

A. ANTENNA FABRICATION

The antenna device has been manufactured using microfabrication techniques available in the clean room of the XLIM laboratory. Briefly, we started with 12.5 mm x 12.5 mm RO4003C substrates metallized on one side with 18-μm thick copper layer defining the ground plane of the antenna. On the non-metallized side of the substrate we deposited firstly a 1-μm thick layer of GeTe using DC magnetron sputtering. The GeTe elements corresponding to the four corners of the patch antenna layer were afterwards patterned using optical lithography and a wet-etching process. Finally, the metallic part of the antenna (main patch and feeding line) was fabricated using a Ti/Au (30/1200 nm) layer obtained by electron-beam evaporation and a photolithographic lift-off method. Finally, a via is drilled through the substrate in order to convey the feeding probe from the connector placed on the metallized side of the device.

Fig. 9 (a) shows the image of the fabricated prototype. The specific states (insulating or conductive) of the GeTe patterns have been optically controlled using direct laser irradiation

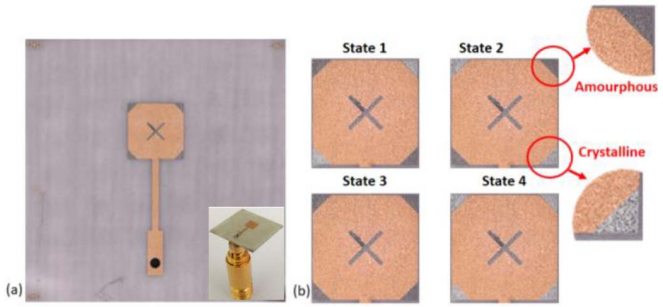

FIGURE 9. Fabricated polarization reconfigurable antenna. (a) Overview of the composite patch with the amorphous GeTe patterns (dark grey color) in the four corners and (b) the different four configurations of the device following locally crystallization of GeTe patterns using laser pulses (light grey colors).

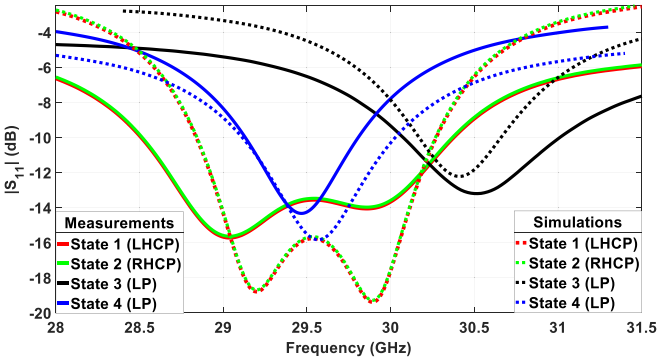

FIGURE 10. Measurements and simulations results of $|S_{11}|$ parameters for different states of GeTe.

with alternating laser pulses LP1 and LP2 in a irradiation scheme identical to the one depicted in Fig. 2. The integration of proximity, contact hard masks placed above the antenna device allowed to address with a high precision the desired areas to be optically modified of the GeTe material. The four different states of the antenna as defined in Table 1, are shown in Fig. 9 (b). One may notice the color changes of GeTe patterns subjected to the insulator-to metal phase change: initially dark grey in the amorphous/insulating state, the patterns are changing to a light grey color, specific to the crystalline/metallic state. The phase change transformation was additionally confirmed by local electrical resistance measurements. Indeed, a thin-film of GeTe was concomitantly deposited on a bare RO4003C substrate during the GeTe deposition step for the antenna device fabrication. The same laser irradiation scheme used for the antenna device for the phase change of the GeTe patches was applied also on the bare substrate, but without the use of the proximity mask. The evaluation of the resistivity changes of GeTe on the RO4003C substrate subsequent to laser irradiation process using a four point resistivity measurement technique allows to record a conductivity of the GeTe in the crystalline state of 3 x 10^5 S/m.

The $|S_{11}|$ parameter, the gain, the radiation pattern and the axial ratio (AR) for the different configurations of the fabricated antenna were measured and the results were compared with the simulations. As mentioned in Section II, the phase changes of GeTe patterns were not performed in-situ, in real time (while the antenna was in measurement or radiating). The measurements were made after each phase change of the GeTe, due to the size of the laser device used which makes it difficult to implement a more compact scheme during our experiments. As indicated before, real-time measurements may be implemented using a dedicated, low-imprint laser system.

B. S PARAMETERS MEASUREMENTS

A SMP-type connector integrated at the back of the antenna allows to excite the microstrip line and measure the antenna performances. $|S_{11}|$ parameters for the States 1, 2, 3 and 4 (as defined in Table 1) are presented in Fig. 10 and show a good impedance matching around 29.5 GHz, as predicted by the simulation.

As expected, the State 3 (when all the GeTe patterns are amorphous) has a working frequency band situated at higher values than the other states (antenna's overall dimensions are smaller). The measured matching bandwidth ($|S_{11}| < -10$ dB) for LHCP and RHCP configurations is 1.9 GHz around 29.5 GHz while it reaches 0.7 GHz around 29.5 GHz for the linear polarization associated with State 4. It is corresponding to 6.4 % of bandwidth for the circular polarization and 2.3 % for the linear one.

It can be observed that States 1, 2 and 4 presents a similar operating frequency band of 0.7 GHz around 29.5 GHz while presenting different polarizations, LHCP, RHCP and LP respectively. Radiation performances of these antenna configurations will be characterized in the next section, in terms of axial ratio (AR), realized gain and total efficiency.

C. RADIATION PERFORMANCES OF THE RECONFIGURABLE DEVICE

A Compact Antenna Test Range (CATR) measurement system going from 8 GHz to 110 GHz, shown in Fig. 11 (a), has been used to evaluate radiation performances of the proposed antenna. The antenna under test (AUT) is shown in Fig. 11 (b) while it is mounted on a SMP-to-K-type connector transition. As can be observed on Fig. 11 (a), the radiation pattern of the antenna is measured in reception configuration.

1) CIRCULAR POLARIZATION CASES

To detail the measurement results, Fig. 12 shows the measured and simulated gains for the LHCP and the RHCP in the State 1 configuration, at two planes ($\varphi = 0°$ and $\varphi = 90°$) and at 29.5 GHz. This is the frequency at which the minimum of the AR is obtained in the LHCP case (State 1) and for which the minimum of the $|S_{11}|$ is obtained in the LP (State 4).

It can be seen that for this State 1, the RHCP gain level is about 20 dB lower than that of LHCP for an angle theta between $-30°$ and $30°$. It is indicating good performances of the circular polarization in this configuration with

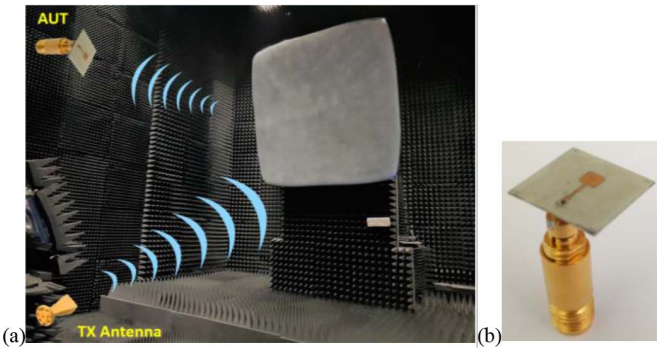

FIGURE 11. (a) Anechoic chamber used for measurements of the (b) fabricated antenna (AUT).

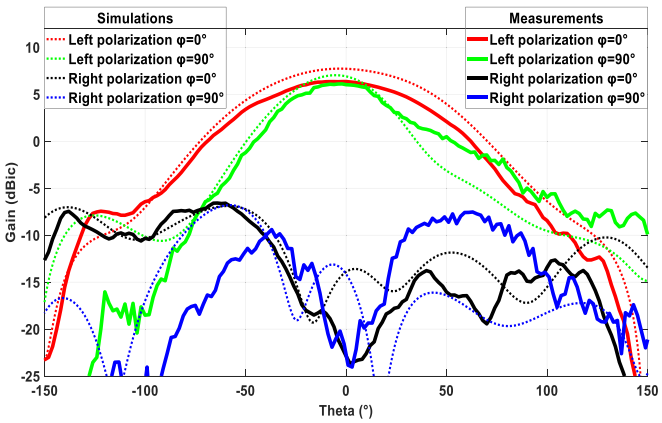

FIGURE 12. Measured and simulated LHCP and RHCP gains for the State 1 (LHCP) at 29.5 GHz.

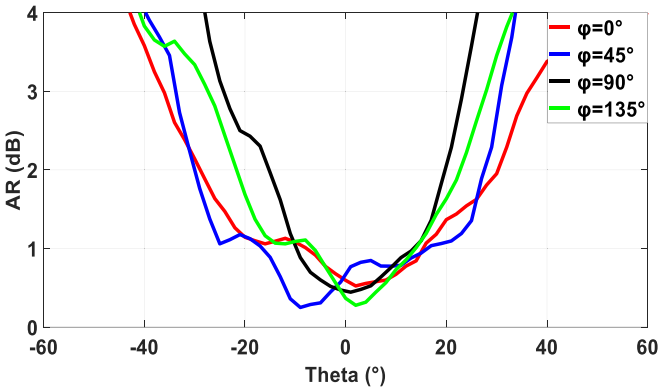

FIGURE 13. Measured axial ratio for the proposed antenna at different φ planes at 29.5 GHz.

a good agreement between the measurement and the simulation. The corresponding measured axial ratio for different φ planes and at 29.5 GHz is represented in Fig. 13. An AR lower than 3 dB is obtained in an angular theta range from $-25°$ to $25°$ for the worst case scenario ($\varphi = 90°$). This AR disturbance in the $\varphi = 90°$ plane is explained by the presence of the coaxial cable included within the CATR measurement system and the connector used for the measurement set-up, and was also verified by simulations.

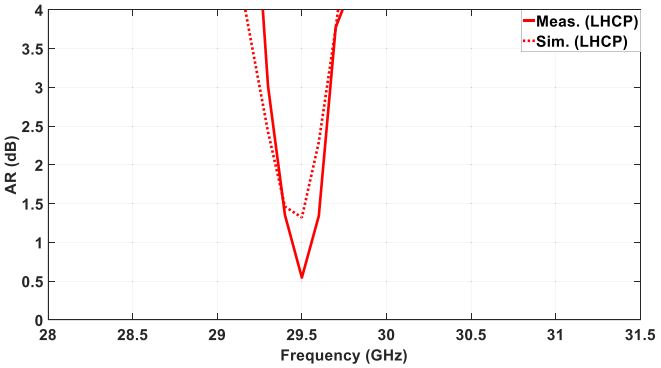

FIGURE 14. Measured and simulated axial ratios of the proposed antenna.

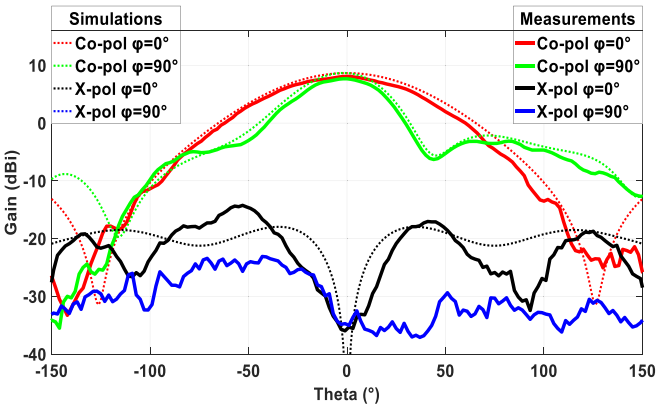

FIGURE 15. Measured and simulated radiation patterns for the proposed antenna in State 4 (LP) at 29.5 GHz.

The boresight ($\varphi = 0°$, $\theta = 0°$) axial ratio can be plotted as a function of the frequency (Fig. 14) and shows an AR of less than 3 dB over a 400-MHz bandwidth around 29.5 GHz, corresponding to 1.7% of bandwidth.

The LHCP State exhibits good performances with an axial ratio bandwidth lower than 3 dB aligned within the impedance matching bandwidth. The RHCP antenna configuration (State 2) is presenting equivalent results due to the antenna's symmetry and therefore is not presented here.

2) LINEAR POLARIZATION CASE

Fig. 15 shows the radiation pattern corresponding to the LP (State 4) in two planes ($\varphi = 0°$ and $\varphi = 90°$) at 29.5 GHz. he level of the cross-polarization is 20 dB lower between $\theta = -45$ and 45 degrees with respect to the co-polarization. A good linear polarization is therefore obtained in this state at 29.5 GHz, i.e., the same frequency than the one corresponding to the LHCP and RHCP cases.

3) PERFORMANCES SUMMARY FOR THE FOUR STATES

To have a complete view on the antenna performances, the directivity, the realized gain and the total efficiency have been measured for the different configurations. As for the previous section, on Fig. 16 are plotted the frequency dependence of the maximum realized gains for States 1 and 4. In the

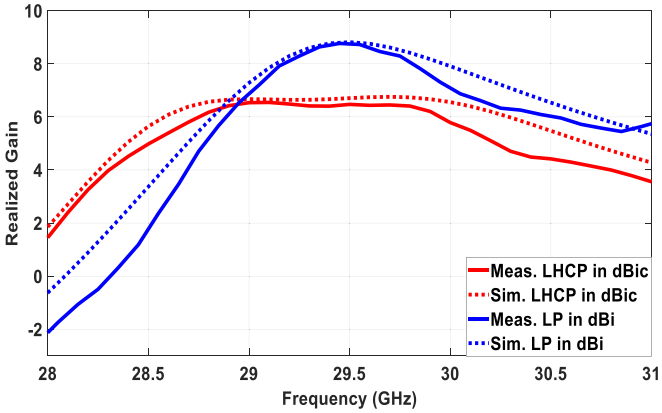

FIGURE 16. Measured and simulated results of maximum realized gain for the circular polarization and for the linear polarization.

TABLE 2. Summary of antenna performance for measured and simulated results.

	BW ($\|S_{11}\|$<-10 dB)	BW (AR<3 dB)	Max. Gain	Tot. Eff. (%)
State 1 Meas. (LHCP)	6.4 %	1.7 %	6.2 dBic	75
State 1 Sim. (LHCP)	5.1 %	1.7 %	6.8 dBic	83
State 2 Meas. (RHCP)	6.4 %	1.7 %	6.2 dBic	75
State 2 Sim. (RHCP)	5.1 %	1.7 %	6.8 dBic	83
State 4 Meas. (LP)	2.3 %	---	8.3 dBi	67
State 4 Sim. (LP)	3.1 %	---	8.6 dBi	78

State 1, the measured realized gain is reaching 6.2 dBic at 29.5 GHz while it is around 8.3 dBi for the State 4. Table 2 summarizes the measured and simulated performances of the device in terms of bandwidth, gain, and total efficiency for the three configurations (LHCP, RHCP and LP cases) where a polarization reconfigurability for a same frequency band around 29.5 GHz is obtained.

As the proposed antenna has been designed and fabricated using GeTe material for the polarization agility. The lower values of measured total efficiencies compared to the simulation results, although acceptable, can be explained by differences in dielectric properties of GeTe obtained on the RO4003C compared with the GeTe material properties used for the simulations (extracted from devices realized on sapphire, low-roughness substrates).

V. CONCLUSION

A hybrid metal-GeTe patch antenna operating around 29.5 GHz was designed for polarization reconfiguration. The fabricated antenna can operate around 29.5 GHz on a linear, left-hand or right-hand circular polarization, depending on the different states (insulating or conductive) of the GeTe material integrated within the metal patch. These states can be conveniently and reversible controlled in a bi-stable manner by single laser pulses.

Thus, we proposed a simple and suitable way to realize antennas operating at millimeter-waves and having variable, on-demand, linear or circular polarization states. The optimization of the global topology of the device will allow the bandwidth increase of the axial ratio in the circular polarization configurations as well as the integration of other reconfigurability functions within the same antenna device (frequency, radiation pattern).

This first demonstration of an optical reconfiguration method of a polarization reconfigurable antenna will open the way for more integrated, in-plane activation schemes using the ability of PCM materials to conveniently modify their electrical properties under optical stimuli.

REFERENCES

[1] W. A. Awan, A. Zaidi, N. Hussain, S. Khalid, Halima, and A. Baghdad, "Frequency reconfigurable patch antenna for millimeter wave applications," in *Proc. Int. Conf. Comput. Math. Eng. Technol. (iCoMET)*, 2019, pp. 1–5.

[2] P.-Y. Qin, Y. J. Guo, Y. Cai, E. Dutkiewicz, and C.-H. Liang, "A reconfigurable antenna with frequency and polarization agility," *IEEE Antennas Wireless Propag. Lett.*, vol. 10, pp. 1373–1376, 2011.

[3] P. K. Li, Z. H. Shao, Q. Wang, and Y. J. Cheng, "Frequency- and pattern-reconfigurable antenna for multistandard wireless applications," *IEEE Antennas Wireless Propag. Lett.*, vol. 14, pp. 333–336, 2014.

[4] Y. I. Abdulraheem, A. S. Abdullah, H. J. Mohammed, B. Mohammed, and R. A. Abd-Alhameed, "Design of radiation pattern reconfigurable 60-GHz antenna for 5G applications," *J. Telecommun.*, vol. 27, no. 2, pp. 7–11, Oct. 2014.

[5] W.-S. Yoon, J.-W. Baik, H.-S. Lee, S. Pyo, S.-M. Han, and Y.-S. Kim, "A reconfigurable circularly polarized microstrip antenna with a slotted ground plane," *IEEE Antennas Wireless Propag. Lett.*, vol. 9, pp. 1161–1164, 2010.

[6] Y. J. Sung, T. U. Jang, and Y.-S. Kim, "A reconfigurable microstrip antenna for switchable polarization," *IEEE Microw. Compon. Lett.*, vol. 14, no. 11, pp. 534–536, Nov. 2004.

[7] H. Wong, K. K. So, K. B. Ng, K. M. Luk, C. H. Chan, and Q. Xue, "Virtually shorted patch antenna for circular polarization," *IEEE Antennas Wireless Propag. Lett.*, vol. 9, pp. 1213–1216, 2010.

[8] K. M.-J. Ho and G. M. Rebeiz, "A 0.9–1.5 GHz microstrip antenna with full polarization diversity and frequency agility," *IEEE Trans. Antennas Propag.*, vol. 62, no. 5, pp. 2398–2406, May 2014.

[9] E. Aloni and R. Kastner, "Analysis of a dual circularly polarized microstrip antenna fed by crossed slots," *IEEE Trans. Antennas Propag.*, vol. 42, no. 8, pp. 1053–1058, Aug. 1994.

[10] E. Herth, N. Rolland, and T. Lasri, "Circularly polarized millimeter-wave antenna using 0-level packaging," *IEEE Antennas Wireless Propag. Lett.*, vol. 9, pp. 934–937, 2010.

[11] E. Arnaud, L. Huitema, R. Chantalat, A. Bellion, and T. Monediere, "Miniaturization of a circular polarized antenna using ferrite materials," in *Proc. 12th Eur. Conf. Antennas Propag. (EUCAP)*, London, U.K., Apr. 2018, p. 5.

[12] A. Crunteanu, L. Huitema, J.-C. Orlianges, C. Guines, and D. Passerieux, "Optical switching of GeTe phase change materials for high-frequency applications," in *Proc. IEEE MTT-S Int. Microw. Workshop Series Adv. Mater. Process.*, Pavia, Italy, Sep. 2017, pp. 1–3.

[13] L. Huitema, J. Leon Valdes, H. Wong, and A. Crunteanu, "Optical switching of GeTe phase change material: Application to a frequency agile millimeter-waves patch antenna," in *Proc. 12th Eur. Conf. Antennas Propag. (EUCAP)*, London, U.K., Apr. 2018, pp. 1–5.

[14] A. Mennai, A. Bessaudou, F. Cosset, C. Guines, P. Blondy, and A. Crunteanu, "Bistable RF switches using Ge2Sb2Te5 phase change material," in *Proc. 18th Eur. Microw. Week (EuMW)*, Paris, France, 2015, pp. 1–4.

[15] N. El-Hinnawy *et al.*, "Substrate agnostic monolithic integration of the inline phase-change switch technology," in *IEEE MTT-S Int. Microw. Symp. Dig.*, San Francisco, CA, USA, 2016, pp. 1–4.

[16] Y. Shim, G. Hummel, and M. Rais-Zadeh, "RF switches using phase change materials," in *Proc. IEEE Int. Conf. Microelectromech. Syst. (MEMS)*, 2013, pp. 237–240.
[17] G. Slovin, M. Xu, R. Singh, T. E. Schlesinger, J. Paramesh, and J. A. Bain, "Design criteria in sizing phase-change RF switches," *IEEE Trans. Microw. Theory Techn.*, vol. 65, no. 11, pp. 4531–4540, Nov. 2017.
[18] R. M. Young *et al.*, "Improvements in GeTe-based phase change RF switches," in *Proc. IEEE/MTT-S Int. Microw. Symp. (IMS)*, 2018, pp. 832–835.
[19] D. Tomer and R. A. Coutu, Jr., "A phase change material for reconfigurable circuit applications," *Appl. Sci.*, vol. 8, no. 1, p. 130, 2018.
[20] X. Sun, E. Thelander, P. Lorenz, J. W. Gerlach, U. Decker, and B. Rauschenbach, "Nanosecond laser-induced phase transitions in pulsed laser deposition-deposited GeTe films," *J. Appl. Phys.*, vol. 116, no. 13, 2014, Art. no. 133501.
[21] W. Gawelda, J. Siegel, C. N. Afonso, V. Plausinaitiene, A. Abrutis, and C. Wiemer, "Dynamics of laser-induced phase switching in GeTe films," *AIP J. Appl. Phys.*, vol. 109, no. 12, 2011, Art. no. 123102.
[22] L. Chau *et al.*, "Optically controlled GeTe phase change switch and its applications in reconfigurable antenna arrays," in *Proc. SPIE. Open Archit./Open Bus. Model Net Centric Syst. Defense Transformation*, 2015, Art. no. 947905.
[23] P. Mahanta, M. Munna, and R. A. Coutu, "Performance comparison of phase change materials and metal-insulator transition materials for direct current and radio frequency switching applications," *Technologies*, vol. 6, no. 2, p. 48, 2018.
[24] S. D. Ha, Y. Zhou, A. E. Duwel, D. W. White, and S. Ramanathan, "Quick switch: Strongly correlated electronic phase transition systems for cutting-edge microwave devices," *IEEE Microw. Mag.*, vol. 15, no. 6, pp. 32–44, Sep./Oct. 2014.
[25] S. Raoux and M. Wuttig, *Phase Change Materials: Science and Applications*. New York, NY, USA: Springer, 2009.
[26] K. Y. Lam, K.-M. Luk, K. F. Lee, H. Wong, and K. B. Ng, "Small circularly polarized U-slot wideband patch antenna," *IEEE Antennas Wireless Propag. Lett.*, vol. 10, pp. 87–90, 2011.
[27] M. Nosrati and N. Tavassolian, "A single feed dual-band, linearly/circularly polarized cross-slot millimeter-wave antenna for future 5G networks," in *Proc. IEEE Int. Symp. Antennas Propag. USNC/URSI Nat. Radio Sci. Meeting*, San Diego, CA, USA, 2017, pp. 2467–2468.
[28] M. S. Nishamol, V. P. Sarin, D. Tony, C. K. Aanandan, P. Mohanan, and K. Vasudevan, "An electronically reconfigurable microstrip antenna with switchable slots for polarization diversity," *IEEE Trans. Antennas Propag.*, vol. 59, no. 9, pp. 3424–3427, Sep. 2011.
[29] K.-F. Tong and T.-P. Wong, "Circularly polarized U-slot antenna," *IEEE Trans. Antennas Propag.*, vol. 55, no. 8, pp. 2382–2385, Aug. 2007.